Biochemical and Biophysical Research Communications 452 (2014) 490–496

Contents lists available at ScienceDirect

Biochemical and Biophysical Research Communications

journal homepage: www.elsevier.com/locate/ybbrc

Snail regulates the motility of oral cancer cells via RhoA/Cdc42/p-ERM pathway

Yao-yin Li, Chuan-Xiang Zhou *, Yan Gao *

Department of Oral Pathology, Peking University School and Hospital of Stomatology, Beijing, PR China

ARTICLE INFO

Article history:
Received 16 August 2014
Available online 27 August 2014

Keywords:
Cell motility
Oral squamous cell carcinoma
Snail
RhoA/Cdc42/p-ERM pathway
Epithelial-to-mesenchymal transition
Metastasis

ABSTRACT

The transcriptional factor Snail has been reported to possess properties related to cancer progression; however, the mechanism for it is not fully understood. Our data showed that Snail knockdown by small interfering RNA in two OSCC cell lines, WSU-HN6 and CAL27, significantly inhibited cell migration and invasion which also resulted in decreased cell motility, such as impaired cell spreading on type I collagen substrate, reduced filopodia, and premature assembly of stress fibers. In addition, Snail-silencing decreased Cdc42 activity but increased RhoA activity, accompanied by the downregulation in both p-ERM expression and cell motility. Meanwhile, endogenous p-ERM was found specifically co-precipitated with activated Cdc42, but not RhoA, and this co-association was decreased by Snail-silencing. The small molecule inhibitors of Rho-associated kinase (Y27632) markedly enhanced Cdc42 activity and the association of p-ERM with activated Cdc42, increasing cell motility remarkably. Using immunohistochemistry, Snail and p-ERM overexpressions were found in OSCC tissues correlated with nodal metastasis and shorter survival. Taken together, these results demonstrate that Snail regulates cell motility through RhoA/Cdc42/p-ERM pathway and may serve as a biomarker to predict prognosis for OSCC patients. Although RhoA and Cdc42 are concurrently regulated downstream of Snail, there is a direct interplay between them, which indicates RhoA has to be inactivated at some point in cell motility cycle.

1. Introduction

Oral and pharyngeal cancer is the sixth lethal cancer worldwide and 90% of oral malignancies are squamous cell carcinomas [1]. The poor prognosis is mainly correlated with metastasis to draining lymph nodes that present in approximately 50% of patients at the time of diagnosis [2]. Since early metastasis occurs frequently in OSCC, extensive efforts are being made to characterize molecular events associated with tumor metastasis and to identify biomarkers for prognosis assessment in OSCC.

In adult epithelium, cells maintain tight contraction and polarization of the actin cytoskeleton, which is indispensible to provide mechanical support for the cells to carry out essential functions like division and movement. However, the orderly cell–cell junction and polarized organization are disturbed in OSCC [3]. Epithelial-to-mesenchymal transition (EMT) is a common phenomenon occurring in tumor invasion and metastasis, during which cancer cells not only change their shape and actin cytoskeleton, but also lose the expression of epithelial markers and acquire mesenchymal signatures [4]. It is known that decreased E-cadherin and increased Vimentin expression is a hallmark of EMT that is regulated by multiple signaling pathways and transcription factors [4]. Snail-related zinc-finger transcriptional repressors (Snail/SNAI1 and Slug/SNAI2) are the most prominent suppressor of E-cadherin transcription that acts by binding to specific E-boxes in the E-cadherin promoter [5]. Meanwhile, actin cytoskeleton remodeling promotes morphological changes and cell migration during EMT, which is also crucial for the invasion and metastasis of cancer cells. It has been reported that actin cytoskeleton rearrangement is controlled by RhoA/Cdc42/Rac1 pathways [6]. RhoA, Rac1, and Cdc42 are three characterized members of Rho GTPases which are small (20–40 KDa) monomeric G proteins belonging to Ras superfamily. When RhoA is activated, actin stress fibers are rearranged to form focal-adhesion, and on the contrary, active Cdc42/Rac1 leads to actin fiber polymerized to form membrane protrusion, enhancing the motility of cancer cells [7]. The ezrin/radixin/moesin (ERM) family is thought to be a cross-linker between plasma membranes and actin-based cytoskeleton which

Abbreviations: EMT, epithelial-to-mesenchymal transition; ERM, ezrin/radixin/moesin; OSCC, oral squamous cell carcinoma; p-ERM, phosphorylated ezrin/radixin/moesin.

* Corresponding authors. Address: Peking University School and Hospital of Stomatology, 22 South Avenue Zhongguancun, Haidian District, Beijing 100081, PR China. Fax: +86 10 62173402.

E-mail addresses: zhoucx2008@126.com (C.-X. Zhou), gaoyan0988@163.com (Y. Gao).

http://dx.doi.org/10.1016/j.bbrc.2014.08.110
0006-291X/

also participates in the regulation of EMT and cell motility [8]. Recently it has been reported that both the Rho GTPases and ERM family are involved in tumor metastasis [9]. However, to our knowledge, there is still no evidence to support the correlation of RhoA/Cdc42/Rac1 pathway with Snail, ERM, and cell motility of OSCC cells.

Based on this information, the aim of this study was to investigate the role of Snail, RhoA/Cdc42/Rac1 and ERM in regulation of cell motility and meanwhile to clarify the crosstalk between them during the progression of OSCC.

2. Materials and methods

2.1. Cell cultures and transfection

Two established OSCC cell lines, WSU-HN6 and CAL27, were kindly donated by the Department of Central Laboratory, Peking University School and Hospital of Stomatology. The cells were incubated in DMEM medium containing 10% fetal bovine serum (FBS) at 37 °C in a 5% CO_2 atmosphere. On-TARGET plus Human SNAI1 siRNA-SMARTpool and control siRNA were obtained from Dharmacon (Thermo Scientific, Lafayette, CO, USA). Transfections with 100 nM SNAI1 siRNA or control siRNA were carried out in both OSCC cells using DharmaFECT transfection reagent according to the manufacturer's instructions.

2.2. Quantitative real-time PCR

The total RNA of transfected cells was extracted by the Tritrol reagent (Invitrogen, Carlsbad, CA, USA) according to the manufacturer's instructions. Then 2 μg of total RNA was reverse transcribed into cDNA using a RT-PCR system (Promega, Madison, WI, USA). The qRT-PCR was carried out using a 7500 real-time PCR system of Applied Biosystems with Fast Start Universal SYBR Green Master (Roche, Indianapolis, IN, USA) according to the manufacturer's instructions. The following primers were used: Snail (forward, 5′-GACTACCGCTGCTCCATTCCA-3′; reverse, 5′-TCCTCTTCATCACTAA TGGGGCTTT-3′); GAPDH (for-ward, 5′-AGAAGGCTGGGGCTCATTTG -3′; reverse, 5′-AGGGGCCATCCACAGTCTTC-3′). All data were normalized to GAPDH expression.

2.3. Western blotting

Each lane was loaded with 30 μg of protein on 10% SDS–PAGE gels. The proteins were then transferred to PVDF membrane (Millipore, Bedford, MA, USA). The membrane was blocked with 10% skim milk for 1 h and then incubated overnight at 4 °C with each primary antibody against its specific protein. The membrane were washed three times and incubated with a 1:10,000 dilution of the secondary antibodies for 1 h and the protein bands were detected with ECL chemiluminescence. Antibodies used were as follows: GAPDH (ZSGB-BIO, Beijing, China), Moesin (abcam, Cambridge, MA, USA), Ezrin (abcam, Cambridge, MA, USA), Radixin (Santa Cruz Biotech, Santa Cruz, CA, USA), phospho-ezrin (Thr567)/radixin (Thr564)/moesin (Thr558) (Cell Signaling Technology, Danvers, MA, USA) and Snail (Bioworld Technology, St. Paul, MN, USA). Densitometric analysis was carried out using ImageJ software.

2.4. Cell immunofluorescence

WSU-HN6 and CAL27 cells were grown on coverslips, fixed with 4% paraformaldehyde for 30 min and then permeabilized with 0.1% Triton X 100 for 5 min. Cytoskeleton were visualized by staining with a 1:500 dilution of fluorescein isothiocyanate (FITC)-conjugated Phalloidin (Cytoskeleton, Denver, CO, USA).

2.5. Wound-healing, invasion and cell spreading assays

The transfected WSU-HN6 and CAL27 cells were seeded onto 6-well plates in DMEM medium with 0.5% FBS. When grown to 90% confluence, the cells were scraped with pipette tip. After that, the cells were incubated in serum-free media. The extent of closure of scratched cells was analyzed by the percentage of the scratched gap closure at each time point.

The invasion of cells was analyzed by 24-well transwell system (Costar, Lowell, MA, USA), pre-coated with Matrigel (BD, San Jose, CA, USA). After being trypsinized and washed, 1×10^4 transfected cells were placed in the upper chamber. Medium containing 20% FBS was placed in the lower chamber as chemoattractant. After incubation at 37 °C, the non-invading cells were removed from the upper surface of the membrane using cotton tipped swabs, and then the cells in the lower surface of the membrane were fixed in 4% paraformaldehyde and stained with crystal violet. The number of invaded cells was counted in 6 fields under a microscope.

Transfected WSU-HN6 and CAL27 cells were seeded onto dishes that were coated with 500 ng/cm^2 type I collagen (BD, San Jose, CA, USA). The status of the spreading cells was observed at each time point.

2.6. Pull-down assays with PAK-GST-PBD and Rhotekin-RBD beads

RhoA/Cdc42/Rac1 activity was assessed by a pull-down assay according to the manufacturer's instructions for RhoA/Cdc42/Rac1 Activation Assay Biochem Kit (Cytoskeleton, Denver, CO, USA). Samples containing the same amount of protein (30 μg) protein from each transfected cell was used for Western blotting quantitation of total RhoA, Cdc42, and Rac1, and 300 μg total protein from each cell was added to 50 μg GST-Rhotekin-RBD beads (for RhoA activation assay) and 10 μg GST-PAK-PBD beads (for Cdc42 and Rac1 activation assay), incubated at 4 °C for 1 h. GTP-bound proteins were collected and then detected by Western blotting analysis.

For co-precipitation experiment, transfected cells were lysed in buffer containing protease inhibitor cocktail tablets, and 100 nM GTPγS or GDP. Lysates were incubated at 4 °C for 30 min and centrifuged at 16,000*g* for 20 min at 4 °C. Supernatants were incubated with GST-PAK-PBD or GST-Rhotekin-RBD beads for 1 h at 4 °C and washed three times with buffer. Bound active RhoA/Cdc42, ERM and p-ERM proteins were collected and then detected by Western blotting.

2.7. Tissue samples and immunohistochemistry

A total of 103 OSCC cases of formalin-fixed paraffin-embedded OSCC samples was derived from the archives of the Department of Oral Pathology, Peking University School and Hospital of Stomatology following the approval of the University Institutional Ethics Committee. Immunohistochemistry was performed using the ChemMate Envision™ system as described elsewhere [10]. Immunostaining was performed by adding the appropriate antibody as follows: phospho-ezrin (Thr567)/radixin (Thr564)/moesin (Thr558) (Cell Signaling Technology, Danvers, MA, USA) and Snail (Bioworld Technology, St. Paul, MN, USA). Adjacent normal mucosa was used as normal control. The immunostaining results were analyzed by two independent pathologists who were blinded for the information of each patient. Reactivity was determined according to the percentage of positive cells: up to 1% positive cells were scored as 0, 2–25% as 1, 26–50% as 2, 51–75% as 3, and over 75% as 4. Intensity was graded as follows: no signal (0), weak (1), moderate (2), and strong (3). A total score of 0–12 was finally calculated and graded as negative (−; score: 0–1), weak (+; 2–4), moderate

(++; 5–8), and strong (+++; 9–12). The score of 0–6 was defined as low positive, and 7–12 was considered as high positive.

2.8. Statistical analysis

SPSS 13.0 (SPSS, Chicago, IL) was used to analyze all data. Chi-squared test or Student *t* test was used to compare the variables between groups. The survival rate of the patients was analyzed with Kaplan–Meier method and the difference between groups was analyzed with the log-rank test. All *P*-values < 0.05 were considered significant.

3. Results

3.1. Snail-silencing reduced the migration and invasion of OSCC cells

To identify the role of Snail in the migration and invasion of OSCC cells, RNA interference (RNAi) strategy was used to knockdown Snail in two OSCC cell lines, WSU-HN6 and CAL27. The expression of Snail at protein and mRNA level was detected, respectively. The result demonstrated Snail siRNA strategy effectively suppressed Snail expression in OSCC cells (Fig. 1A). To test the effect of Snail knockdown in cell invasion in WSU-HN6 and CAL27, Transwell Assay indicated that Snail-silenced cells showed a 2–3 fold decrease in gel invasion compared with the Control siRNA counterpart ($P < 0.05$) (Fig. 1B). Furthermore, it was observed that Snail knockdown in OSCC cells significantly reduced cell migration from the edge of the wound after scratching ($P < 0.05$) (Fig. 1C).

3.2. Snail-silencing suppressed the spreading of OSCC cells

To investigate whether Snail-silencing down-regulated the motility of OSCC cells through cytoskeleton regulation, the cell spreading experiment was performed. Both the Snail-silenced cells and the control counterpart did not spread at 6 h post-transfection, seeded in culture dishes precoated with type I collagen. However, 24 h after seeding, the spreading area of mock-transfected cells was much larger than those of Snail-silenced cells (Fig. 1D). Then the actin cytoskeleton was stained with phalloidin in transfected cells to further investigate the role of Snail in cytoskeleton reconstruction. Immunofluorescence images revealed that the number of filopodia reduced in Snail-silenced cells, compared with mock-transfected cells (Fig. 1E).

3.3. Snail regulated cytoskeleton via RhoA/Cdc42/p-ERM pathway

In the present study, Snail-silencing reduced the expression of ERM family and its phosphorylated form (p-ERM) (Fig. 2A). To determine whether Snail affect the status of RhoA/Cdc42/Rac1,

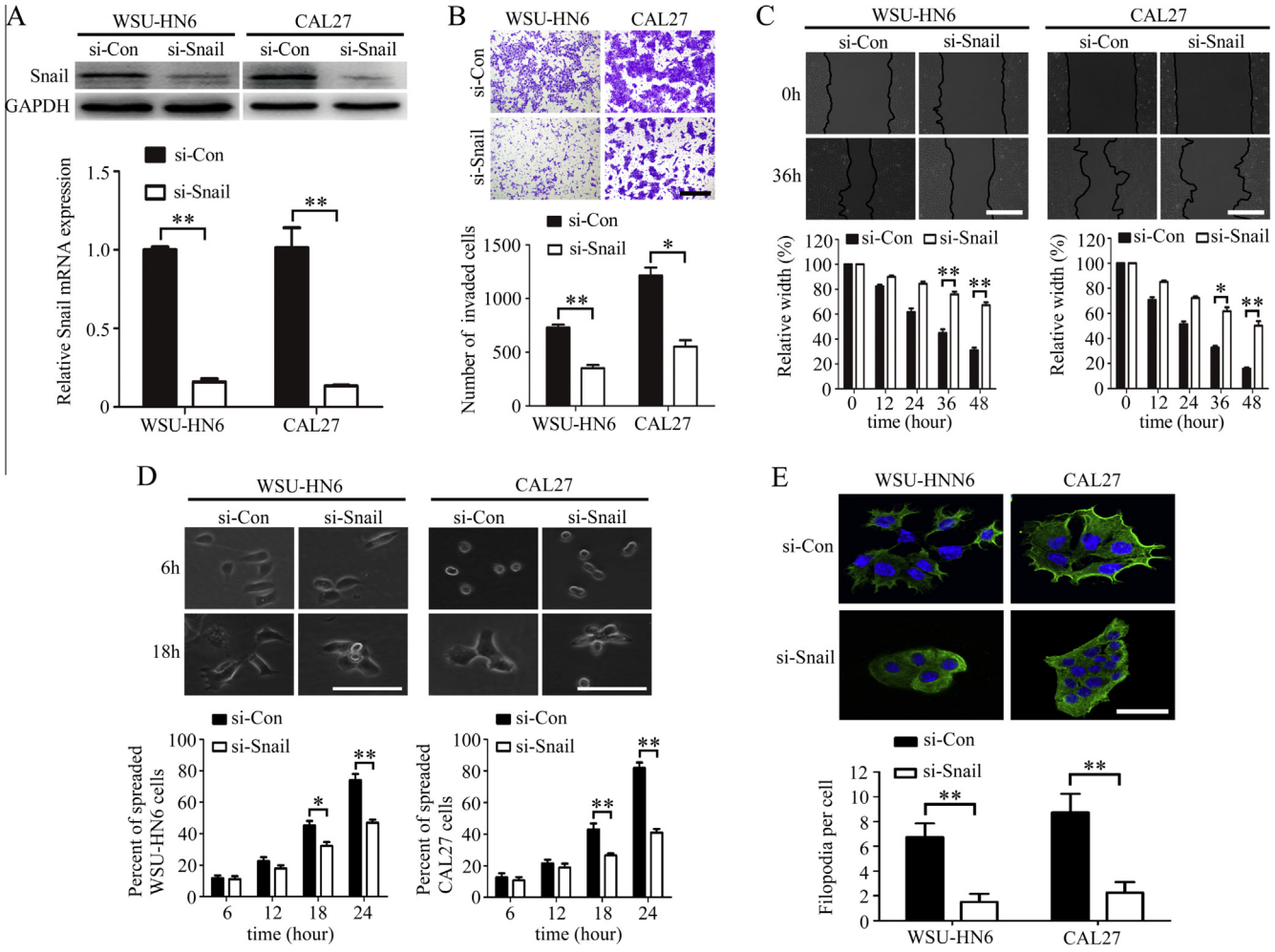

Fig. 1. Effect of Snail-silencing on the motility of OSCC cells. (A) WSU-HN6 and CAL27 were transfected with Control siRNA and Snail siRNA, and the expression of Snail decreased significantly both in mRNA and protein level by Snail siRNA. (B) The invasion of Snail-silenced OSCC cells was measured by Transwell assay. Bar, 400 μm. (C) The migration of Snail-silenced OSCC cells was measured by Wound-healing assay. Bar, 400 μm. (D) The area of spreaded Snail-silenced OSCC cells was measured by cell spreading assay. Bar, 100 μm. (E) The filopodia (defined as membrane protrusion of >5 μm length) of Snail-silenced OSCC cells was stained with phalloidin. Bar, 50 μm. *, represents $P < 0.05$; **, represents $P < 0.01$.

GTP-bound RhoA/Cdc42/Rac1 was investigated by pull-down assay. The level of active GTP-Cdc42 was found decreased significantly in Snail-silenced cells, but the active GTP-RhoA increased markedly unexpectedly, and the status of Rac1 was not affected (Fig. 2B). Furthermore, to determine whether a hierarchy of cross-talk between RhoA and Cdc42 involved in Snail-regulated cell migration, the transfected OSCC cells were treated with small molecule inhibitors of Rho-associated kinase (Y27632). It was found that inhibition of RhoA markedly increased Cdc42 activity in both Snail-silenced and mock-transfected cells (Fig. 2B) and reversed the downregulation of cell migration and invasion by Snail knockdown (Fig. 3A and B).

In order to detect the precise relationship between RhoA/Cdc42 complex and ERM family, co-precipitation experiment was performed. When the lysates of the transfected cells were incubated with GST-PAK-PBD beads that specifically bound to GTP-Cdc42 (activated Cdc42), endogenous p-ERM was found specifically co-precipitated with GTP-Cdc42, but no co-precipitation of p-ERM with RhoA was found when lysates were incubated with GST-Rhotekin-RBD beads, and this co-association of p-ERM and GTP-Cdc42 was decreased by Snail-silencing (Fig. 2C). Although no direct interplay was found between RhoA and p-ERM, Y27632 markedly enhanced Cdc42 activity and augmented the association of p-ERM with activated Cdc42 (Fig. 2C), which was accompanied

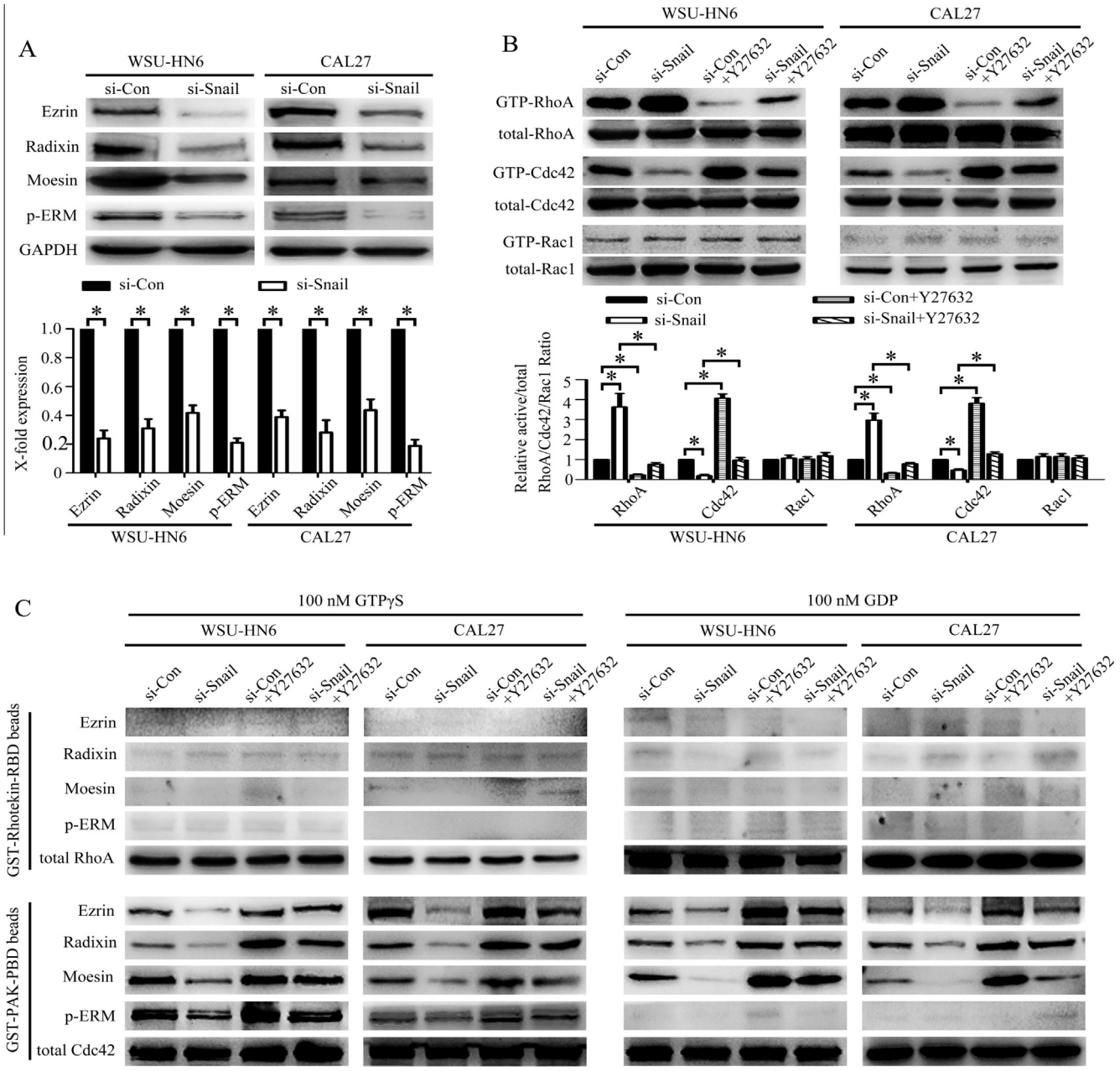

Fig. 2. Snail meditated the motility of OSCC cells via RhoA/Cdc42/p-ERM pathway. (A) WSU-HN6 and CAL27 were transfected with Control siRNA and Snail siRNA on day 0, then harvested on day 2 post-transfection. The ERM and p-ERM protein levels were measured by Western blotting (upper panel, $n = 3$). Quantification of the expression of the ERM and p-ERM protein by densitometric analysis with ImageJ software (lower panel, $n = 3$). (B) OSCC cells were treated with Snail siRNA regents and/or small molecule inhibitors of Rho-associated kinase (Y27632). The treated OSCC cells were lysated and incubated with GST-PAK-PBD beads and GST-Rhotekin-RBD beads, respectively. Western blotting was used to detect the activity of GTP bound RhoA/Cdc42/Rac1 (upper panel, $n = 3$). Quantification of the activity of GTP bound RhoA/Cdc42/Rac1 normalized to total RhoA/Cdc42/Rac1 by densitometric analysis with ImageJ software (lower panel, $n = 3$). (C) OSCC cells were treated with Snail siRNA regents and/or Y27632. Cell lysates were incubated with GST-PAK-PBD beads and GST-Rhotekin-RBD beads in the presence of 100 nM GTPγS or GDP. Bound proteins were probed for ERM and p-ERM protein using Western blotting. (A–B) All data are means ± SE from triplicate experiments. ∗, represents $P < 0.05$.

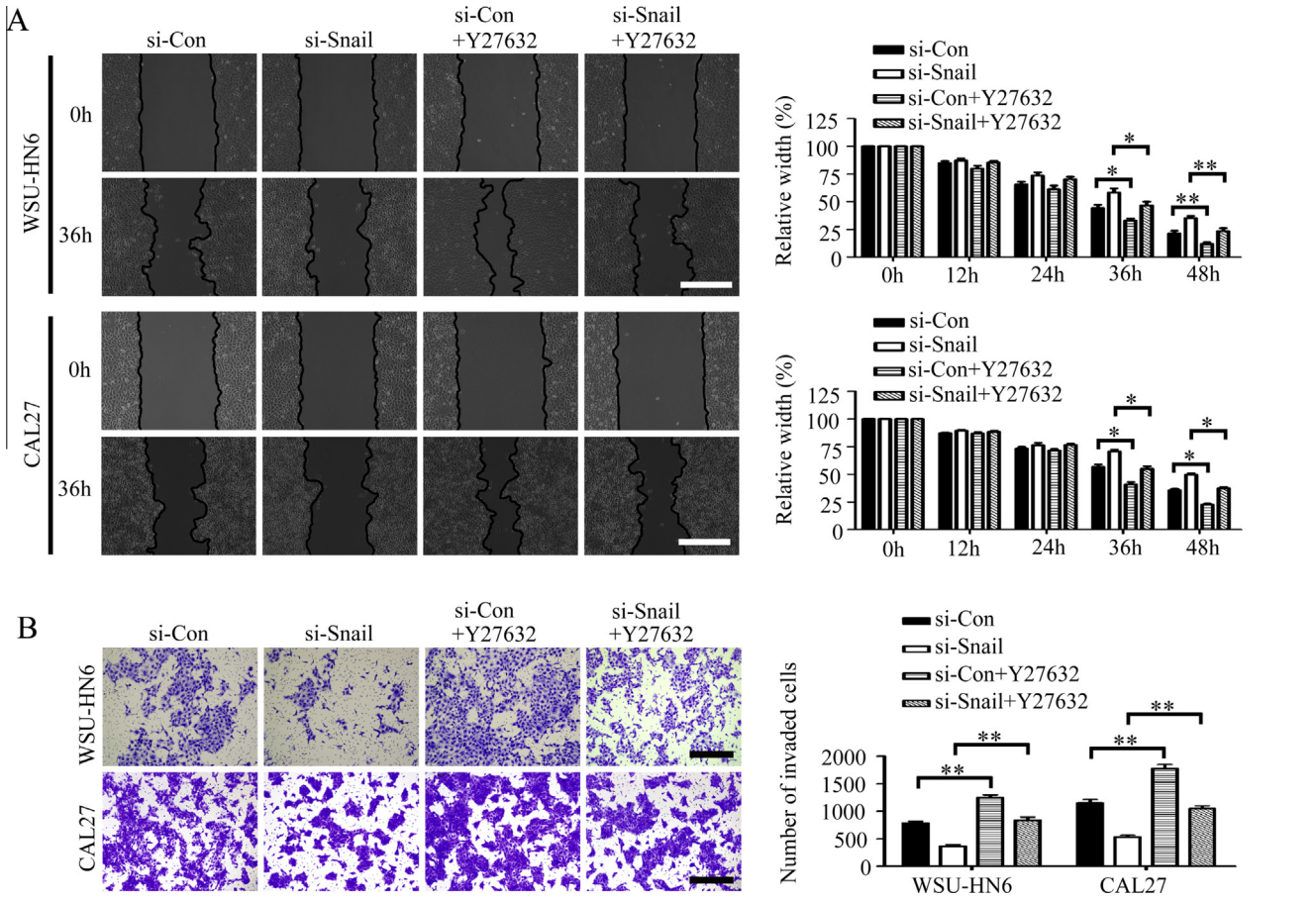

Fig. 3. Small molecule inhibitors of Rho-associated kinase (Y27632) reversed the downregulation of cell motility by Snail knockdown. (A) The migration of OSCC cells treated with Snail siRNA and/or Y27632 was measured by Wound healing assay. Bar, 400 μm. (B) The invasion of OSCC cells treated with Snail siRNA and/or Y27632 was measured by Transwell assay. Bar, 400 μm. (A–B) All data are means ± SE from triplicate experiments. ∗, represents $P < 0.05$; ∗∗, represents $P < 0.01$.

by the remarkably increased cell migration and invasion (Fig. 3A and B). The binding of p-ERM with Cdc42 depended on the presence of GTPγS which did not occur in the presence of GDP (Fig. 2C).

3.4. Overexpression of Snail and phospho-ezrin/radixin/moesin in OSCC tissues was observed and related to nodal metastasis and shorter survival

A representative example of hematoxylin and eosin and immunohistochemical staining for Snail and p-ERM in normal oral tissue and 103 OSCC cases is shown in Fig. 4A. The relationship between Snail and p-ERM expression with clinicopathologic characteristics are summarized in Table 1. No statistically significant association was found between Snail and p-ERM expression with gender, age, location, tumor size and differentiation. However, Snail and p-ERM expression tended to be significantly associated with nodal metastasis (Table 1). In addition, tumor cells with enhanced Snail also showed increased p-ERM expression with a Pearson correlation coefficient ($r = 0.511$, $P < 0.001$) (Fig. 4B). When combined with the expression of Snail and p-ERM, significant poorer survival rates were found in the patients with high expression of both Snail and p-ERM (p-ERM high/Snail high), compared with those with low expression of p-ERM and high expression of Snail (p-ERM low/Snail high) ($P = 0.016$) (Fig. 4C).

4. Discussion

Previous studies have proved Snail promotes tumor progression through regulating EMT in a variety of cancers [11]. To further determine the role of Snail in the invasion and metastasis of OSCC cells, RNA interference was used to knockdown Snail in two OSCC cell lines, WSU-HN6 and CAL27. We found that Snail knockdown in OSCC cells resulted in increased E-cadherin and decreased Vimentin expression (data not shown). Furthermore, the Snail-silenced cells showed a significant reduced cell migration and invasion, which indicates that Snail regulates EMT and promotes tumor invasion and metastasis in OSCC. Meanwhile, the remodeling of dynamic filamentous cytoskeleton is considered as the primary step for cell migration and promotes morphological changes during EMT [12]. To investigate whether Snail silencing downregulated cell invasion and migration through cytoskeleton regulation, the cell spreading experiment was performed and it was found that Snail knockdown caused an impaired cell spreading on type I collagen substrate. Since the formation of filopodia affects cell spreading significantly, the cytoskeleton was then stained with phalloidin in the transfected cells, and it was observed Snail-silencing suppressed the formation of filopodia, which demonstrated the involvement of Snail in cytoskeleton reconstruction.

RhoA, Cdc42, and Rac1 are most characterized members of Rho GTPases which play a pivotal role in both cell adhesion and the cytoskeleton remodeling [13]. In our present study, pull-down assay demonstrated the level of Cdc42 activity was found significantly decreased in Snail-silenced cells. It was found that Cdc42−/− embryonic fibroblast cells could not form functional filopodia, which undermined polarity establishment and cell migration [14]. Our data showed Snail knockdown reduced the activity of Cdc42, accompanied by the decrease in both filopodia formation and cell motility, which indicated Snail might control

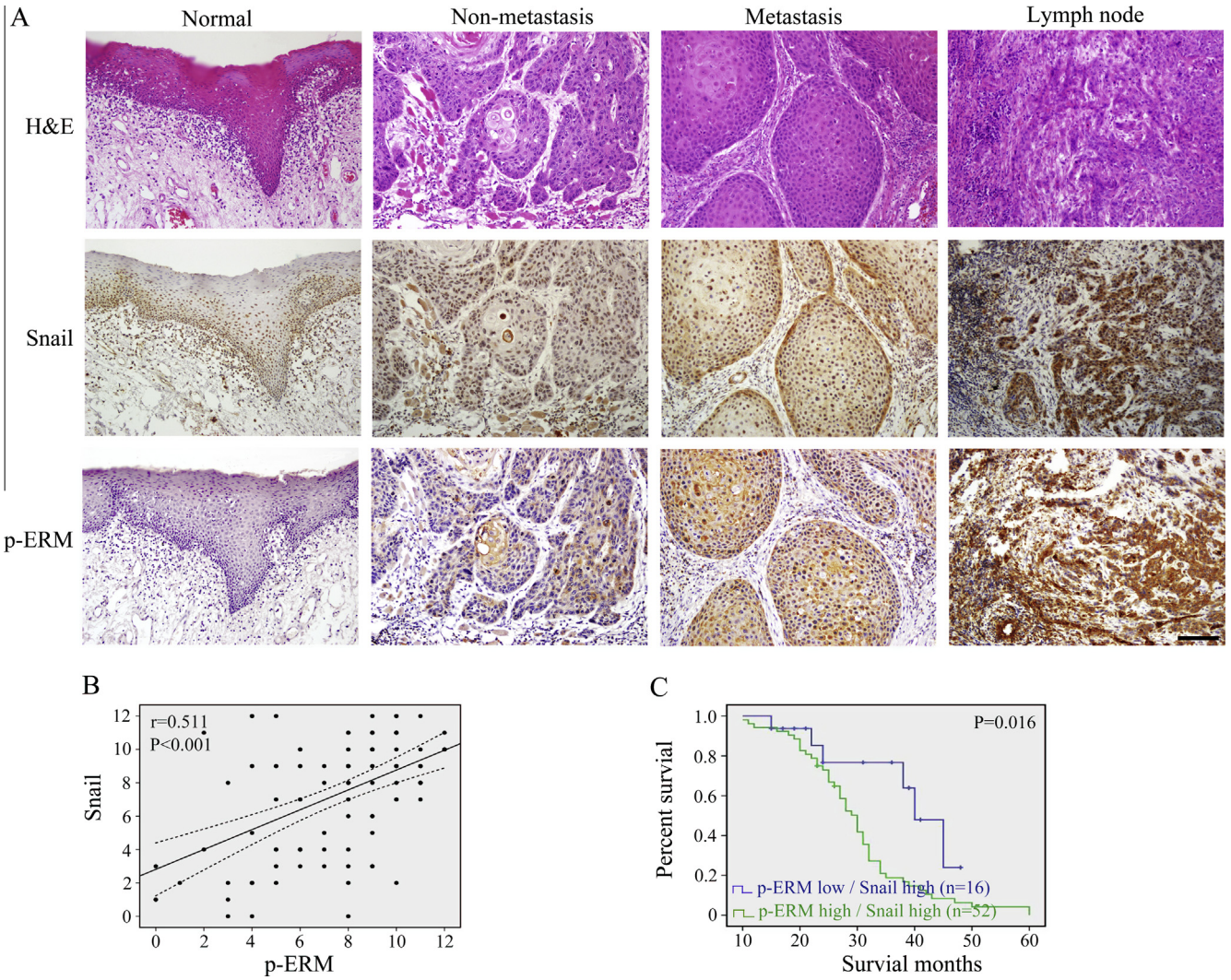

Fig. 4. Analysis of Snail and p-ERM staining in human OSCC samples. (A) Hematoxylin and eosin (H&E) and immunohistochemical staining for Snail and p-ERM staining in normal epithelial, non-metastasis OSCC, primary tumor of OSCC with metastasis and lymph node with metastatic cancer cells. Bar, 100 μm. (B) The association between Snail and p-ERM was assessed using Pearson correlation coefficient. (C) The Kaplan–Meier estimate of 5-year survival rate in OSCC patients according to Snail and p-ERM expression.

cell motility through regulating the activity of Cdc42. Meanwhile, in contrast to Cdc42, active RhoA was found increased markedly in Snail-silenced cells unexpectedly. A positive role of RhoA in cell migration and invasion has been reported in many cell systems [15]; however, the decrease in cell motility due to constitutive activation of RhoA has also been described. Ispanovic et al described the increasing Cdc42 activity caused the same effect on MMP-2 activation as inhibition of RhoA activity, and Cdc42 activation suppressed basal RhoA activity [16]. Nawal Bendris et al showed the activity of RhoC, Cdc42 and Rac1 was inverse with RhoA activity during EMT [17]. As cross talk even the opposing roles between the Rho-GTPases have been reported, we hypothesized although RhoA and Cdc42 might be concurrently regulated downstream of Snail, a direct interplay between RhoA and Cdc42 also exists in our OSCC cell system. To investigate the cross talk between RhoA and Cdc42 and its role in regulation of cell motility, RhoA activity was effectively suppressed by the small molecule inhibitors of Rho-associated kinase (Y27632). Our data showed inhibition of RhoA markedly increased Cdc42 activity and cell motility in both Snail-silenced and control cells, which also partially reversed the decline in cell motility caused by Snail knockdown. In line with our findings, Khalil et al found the expression of a dominant active RhoA inhibited cell motility, and a decrease in RhoA activation was observed specifically evident as the cell retracted its tail to move forward [18], which indicates that RhoA has to be inactivated at some point in the cell motility cycle for the cells to move efficiently.

In addition, it has been reported that the ezrin–radixin–moesin (ERM) family of membrane-cytoskeleton linker proteins regulate many important cellular functions, including cell migration [19] and morphology [20]. In the present study, it was found that Snail-silencing not only suppressed the expression of ERM, but also inhibited its phosphorylation. Recently it has been reported Rho GTPases are involved in the activation of ERM family and ERM-mediated cell motility [21]. In the present study, endogenous p-ERM was found specifically co-precipitated with activated Cdc42, but not RhoA, and this co-association was decreased by Snail-silencing. Although no direct interplay was found between RhoA and p-ERM, Y27632 markedly enhanced Cdc42 activity and augmented the association of p-ERM with activated Cdc42, which was accompanied by the remarkably increased cell motility. Furthermore, we illustrated that high expression of Snail were significantly correlated with increased p-ERM expression in a large series of 103 OSCC cases. Meanwhile, high expression of Snail and

Table 1
Relationship between Snail and p-ERM expression and clinicopathologic features in 103 oral squamous cell carcinoma (OSCC) patients.

Features	Number	Immunoreactivity of Snail		*P*-value	Immunoreactivity of p-ERM		*P*-value
		Low	High		Low	High	
Age(years)				0.213			0.42
⩽60	50	14	36		16	34	
>60	53	21	32		21	32	
Gender				0.068			0.297
Male	57	15	42		23	34	
Female	46	20	26		14	32	
Size(cm)				0.09			0.669
⩽4	78	30	48		35	43	
>4	25	5	20		10	15	
Location				0.537			0.969
Tongue	38	15	23		14	24	
Gingival	26	9	17		10	16	
Buccal	23	8	15		8	15	
Others	16	3	13		5	11	
Differentiation				0.395			0.22
Low	32	13	19		14	18	
Middle	40	12	28		10	30	
High	31	14	17		12	19	
Lymph node				<0.001**			0.024*
pN^-	63	32	31		28	35	
pN^+	40	3	37		9	31	

Data were analyzed using the Chi-squared test.
* represents $P < 0.05$.
** represents $P < 0.01$.

p-ERM indicated poorer prognosis for OSCC patients. These results showed Snail and p-ERM play potential roles in OSCC progression.

In summary, our data demonstrate Snail regulates cell motility through RhoA/Cdc42/p-ERM pathway and promotes tumor invasion and metastasis in OSCC. Although RhoA and Cdc42 are concurrently regulated downstream of Snail, inhibition of RhoA can increase Cdc42 activity directly and enhance the association of p-ERM with activated Cdc42, promoting Snail-mediated cell motility and indicating that RhoA has to be inactivated at some point in cell motility cycle.

Acknowledgment

This study was supported by the National Nature Science Foundation of China (No. 30973338).

References

[1] S. Warnakulasuriya, Global epidemiology of oral and oropharyngeal cancer, Oral Oncol. 45 (2009) 309–316.
[2] S.Y. Kim, S.Y. Nam, S.H. Choi, K.J. Cho, J.L. Roh, Prognostic value of lymph node density in node-positive patients with oral squamous cell carcinoma, Ann. Surg. Oncol. 18 (2011) 2310–2317.
[3] W.G. Stetler-Stevenson, S. Aznavoorian, L.A. Liotta, Tumor cell interactions with the extracellular matrix during invasion and metastasis, Annu. Rev. Cell Biol. 9 (1993) 541–573.
[4] A. Voulgari, A. Pintzas, Epithelial–mesenchymal transition in cancer metastasis: mechanisms, markers and strategies to overcome drug resistance in the clinic, Biochim. Biophys. Acta 1796 (2009) 75–90.
[5] B. De Craene, F. van Roy, G. Berx, Unraveling signalling cascades for the Snail family of transcription factors, Cell. Signal. 17 (2005) 535–547.
[6] G. Pawlak, D.M. Helfman, Cytoskeletal changes in cell transformation and tumorigenesis, Curr. Opin. Genet. Dev. 11 (2001) 41–47.
[7] G.A. Wildenberg, M.R. Dohn, R.H. Carnahan, M.A. Davis, N.A. Lobdell, J. Settleman, A.B. Reynolds, P120-catenin and p190RhoGAP regulate cell-cell adhesion by coordinating antagonism between Rac and Rho, Cell 127 (2006) 1027–1039.
[8] S. Tsukita, S. Yonemura, ERM (ezrin/radixin/moesin) family: from cytoskeleton to signal transduction, Curr. Opin. Cell Biol. 9 (1997) 70–75.
[9] A. Halon, P. Donizy, P. Surowiak, R. Matkowski, ERM/Rho protein expression in ductal breast cancer: a 15 year follow-up, Cell. Oncol. (Dordr.) 36 (2013) 181–190.
[10] M. Tsuneki, M. Yamazaki, J. Cheng, S. Maruyama, T. Kobayashi, T. Saku, Combined immunohistochemistry for the differential diagnosis of cystic jaw lesions: its practical use in surgical pathology, Histopathology 57 (2010) 806–813.
[11] J. Yang, R.A. Weinberg, Epithelial–mesenchymal transition: at the crossroads of development and tumor metastasis, Dev. Cell 14 (2008) 818–829.
[12] H. Yamaguchi, J. Condeelis, Regulation of the actin cytoskeleton in cancer cell migration and invasion, Biochim. Biophys. Acta 1773 (2007) 642–652.
[13] A. Murali, K. Rajalingam, Small Rho GTPases in the control of cell shape and mobility, Cell. Mol. Life Sci. 71 (2013) 1703–1721.
[14] L. Yang, L. Wang, Y. Zheng, Gene targeting of Cdc42 and Cdc42GAP affirms the critical involvement of Cdc42 in filopodia induction, directed migration, and proliferation in primary mouse embryonic fibroblasts, Mol. Biol. Cell 17 (2006) 4675–4685.
[15] K.J. Jeong, S.Y. Park, K.H. Cho, J.S. Sohn, J. Lee, Y.K. Kim, J. Kang, C.G. Park, J.W. Han, H.Y. Lee, The Rho/ROCK pathway for lysophosphatidic acid-induced proteolytic enzyme expression and ovarian cancer cell invasion, Oncogene 31 (2012) 4279–4289.
[16] E. Ispanovic, D. Serio, T.L. Haas, Cdc42 and RhoA have opposing roles in regulating membrane type 1-matrix metalloproteinase localization and matrix metalloproteinase-2 activation, Am. J. Physiol. Cell Physiol. 295 (2008) C600–C610.
[17] N. Bendris, N. Arsic, B. Lemmers, J.M. Blanchard, Cyclin A2, Rho GTPases and EMT, Small GTPases 3 (2012) 225–228.
[18] B.D. Khalil, M. El-Sibai, Rho GTPases in primary brain tumor malignancy and invasion, J. Neurooncol. 108 (2012) 333–339.
[19] M.A. del Pozo, M. Vicente-Manzanares, R. Tejedor, J.M. Serrador, F. Sanchez-Madrid, Rho GTPases control migration and polarization of adhesion molecules and cytoskeletal ERM components in T lymphocytes, Eur. J. Immunol. 29 (1999) 3609–3620.
[20] T.C. Dickson, C.D. Mintz, D.L. Benson, S.R. Salton, Functional binding interaction identified between the axonal CAM L1 and members of the ERM family, J. Cell Biol. 157 (2002) 1105–1112.
[21] M.A. Haas, J.C. Vickers, T.C. Dickson, Rho kinase activates ezrin–radixin–moesin (ERM) proteins and mediates their function in cortical neuron growth, morphology and motility in vitro, J. Neurosci. Res. 85 (2007) 34–46.